DESIGN OF MULTIPURPOSE DISPERSIVE SECTION AT PITZ*

S. Khodyachykh†, J. Bähr, M. Krasilnikov, A. Oppelt, L. Staykov, F. Stephan
(DESY, Zeuthen, Germany),
T. Garvey (LAL, Orsay, France), D. Lipka (BESSY GmbH, Berlin, Germany),
J. Rönsch (University of Hamburg, Hamburg, Germany)

Abstract

A detailed knowledge of the parameters of a high-brightness electron beam is of major importance for evaluating the performance of a free electron laser using the beam. Therefore, a full characterization of the beam parameters is required during the commissioning of RF photo injectors. As one important contribution to fulfill this task, a multi-purpose high energy dispersive arm (HEDA1) for electron energies up to 40 MeV is presently under construction at the Photo Injector Test Facility at DESY in Zeuthen (PITZ). The dispersive section is designed such that it will combine the functionality of 1) an electron spectrometer, 2) a device for characterization of the longitudinal phase space, and 3) a transverse slice emittance measuring system. The HEDA1 consists of a 180° dipole magnet (C-Bend), followed by removable slit, a quadrupole magnet, and a screen station with a read-out for the streak camera. Design considerations and the detailed lay out of the high-energy dispersive section are presented.

INTRODUCTION

The Photo-Injector Test Facility at DESY in Zeuthen (PITZ) is an electron accelerator which was built by Deutsches Elektronen-Synchrotron (DESY) in collaboration with international partners with the goal to develop and to optimize high brightness electron sources suitable for SASE FEL operation.

The PITZ facility consists of a 1.5 cell L-band RF gun, a photo-cathode laser system, a normal-conducting booster cavity and a diagnostic section. Being an operational machine showing pioneering results in achieving of high-charge low-emittance electron beams for electron bunch trains [1], PITZ is still under development. The beam line which has a present length of about 13 meters will be extended up to about 21 meters within the next two years. Many additional diagnostics components will be added to the present layout. Together with the deflecting cavity [2], the phase space tomography module [3] and the second high-energy dispersive arm (HEDA2), HEDA1 will extend the existing diagnostics system of the photo injector. The scope of the present paper is the multi-purpose high energy dispersive arm (HEDA1). The dispersive section is designed to combine the functionality of (i) an electron spectrometer, (ii) a device for characterization of the longitudinal phase space, and (iii) a transverse slice emittance measuring system.

SETUP

The layout of the dispersive section HEDA1 is schematically shown in Fig 1.

The heart of the dispersive section is a 180° dipole magnet having the bending radius of 300 mm. The bending radius has been chosen as a compromise between the space requirements and momentum resolution on the one hand and the ability of the spectrometer to operate within the large range of gun and booster parameters. Being deflected in vertical plane, the electron beam enters the dispersive arm which goes below the main beam line parallel to it. The dispersive arm includes a pumping port combined with a removable slit mask, a quadrupole magnet Q_1 for the slice emittance measurements, a drift space of 600 mm followed by two screen stations (for simplicity only one is shown) and by a beam dump. For measuring of the bunch charge an integrating current transformer (ICT) is foreseen between the two screen stations (not shown).

For the reasons described in the following sections additional components which contribute to the measurements at HEDA are located in the main beam line. These are the quadrupole magnet Q_2 and the screen station S_2 placed up- and downstream to the dipole magnet D, respectively.

The main advantage of the 180-degree spectrometer is the simplicity to reconstruct the momentum distribution [4]. One uses the screen S_2 in the straight section and measures the contribution from the transverse beam size and divergence, which can be de-convoluted with the measured spectrum to obtain the pure momentum distribution. This can be illustrated by comparing of the transport matrix M_D (describing the transport of the electron beam between the position of the quadrupole magnet Q_2 and the screen S_1) with the matrix M_S which corresponds to the drift between Q_2 and the screen S_2. The matrices in thin lens approximation have the form

$$M_D = \begin{pmatrix} -1 & -l_1 - l_2 & 2\rho \\ 0 & -1 & 0 \\ 0 & 0 & 1 \end{pmatrix} M_S = \begin{pmatrix} 1 & l_1 + l_2 & 0 \\ 0 & 1 & 0 \\ 0 & 0 & 1 \end{pmatrix} \quad (1)$$

where ρ is the bending radius of the dipole magnet and lengths l_1 and l_2 are defined in Fig 1.

The transverse coordinates of the i-th electron can be described by a vector $\vec{y_i} = (y_i, y_i', p_i/\langle p \rangle)^T$, where y_i is the

* This work has partly been supported by the European Community, contracts RII3-CT-2004-506008 and 011935, and by the 'Impuls- und Vernetzungsfonds' of the Helmholtz Association, contract VH-FZ-005.

† sergiy.khodyachykh@desy.de

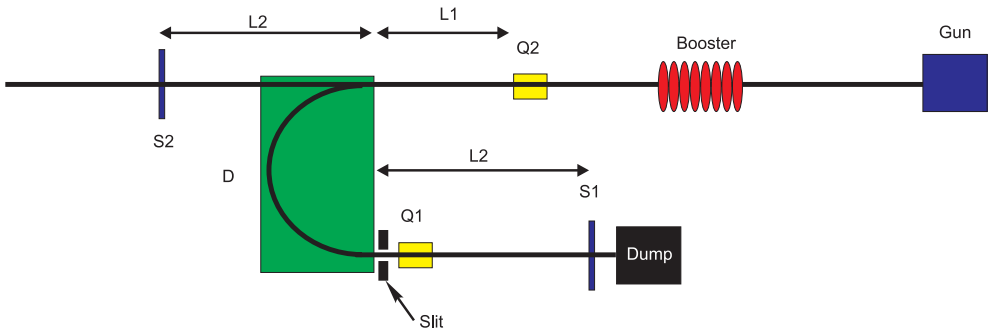

Figure 1: Simplified layout of PITZ with the first high energy dispersive section.

transverse position, y_i' is the divergency and $p_i/\langle p\rangle$ is the relative momentum. Assuming the electron with the coordinate y_0 is transported through the spectrometer it will get the transverse coordinate on the screen S_1 which is described by the first component of vector $\vec{y}_1 = M_D\vec{y}_0$. The shift of the particle with respect to the reference trajectory is thus defined not only by the relative momentum of the particle, but also by it initial transverse offset and divergency. To exclude these two contributions one uses the measurements on the screen S_2 where only initial coordinate and initial divergency define the position of the particle (compare M_{11} and M_{12} elements of matrices in Eq.1). Moreover, by focusing the beam on the screen S_2 with the help of the quadrupole magnet Q_2 one can control the resolution of the momentum measurement.

Beam momentum and momentum spread depends strongly on the machine parameters. It is very sensitive to the RF phases of the gun and of the booster. Because of the large dispersion of the dipole magnet the spot sizes on the screen S_1 are expected to be very large, especially in cases of far off-crest RF phases. Figure 2 shows the dependence of the vertical beam size on the screen S_1 as a two dimensional function of the gun and booster phases. The aperture of the quadrupole magnet Q_1 (80 mm) defines the transversal acceptance of the dispersive section. Thus, using HEDA1 measurements within the range of $-35...35°$ of booster phases will be possible in single shot. For larger off-crest phases a scan of dipole current will be used.

LONGITUDINAL PHASE SPACE

Very important information for the understanding of the photo-injector can be gained by studying the electron distribution in the longitudinal phase space, when the electron momentum is measured as a function of its longitudinal position within the bunch. For this purpose one of the screen stations will be equipped with an aerogel screen used as a Cherenkov radiator and a read-out for the streak-camera.

Figure 3 (a) shows the results of numerical simulation of the longitudinal phase space using the code ASTRA [7] at the entrance of the dipole magnet. The particles were tracked through the dipole using the matrix formalism, similar to that described in previous section, but using 6×6 transport matrix. The longitudinal phase space re-

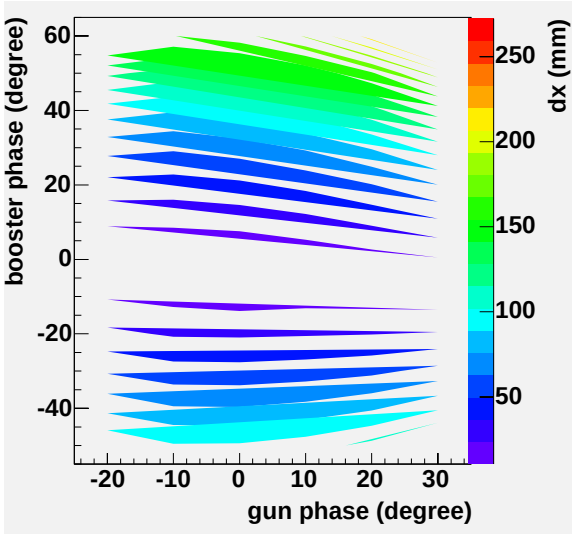

Figure 2: The total beam size in dispersive plane on screen S_1 as a function of gun and booster phases.

constructed on the screen S_1 of the dispersive section after the drift having the length of a 1 m is shown in Fig. 3 (b). A correction of the influence from the matrix element M_{56} [6] was applied in Fig. 3 (c). Figure 3 (d) shows the momentum distribution as a projection of Fig. 3 (a) in red and 3 (c) in blue.

A comparison of the initial and the reconstructed values of mean momentum $\langle p\rangle$, momentum spread p_{rms} and longitudinal emittance ϵ_l are shown in the following table. The

	$< p >$ (MeV)	p_{rms} (keV)	ϵ_l (π keV mm)
(a)	18.3111	36.6	75.99
(c)	18.3109	49.0	105.08
$(a-c)/a$	-0.0009%	33.8%	38.3%

results in Fig. 3 and table were done without quadrupole. These results could be improved by applying deconvolution with known beam size at S_2. However, this procedure unnecessary complicates data analysis comparing to the method discussed below.

The simulations were repeated using a quadrupole triplet 4.5 m downstream the photocathode in order to focus the

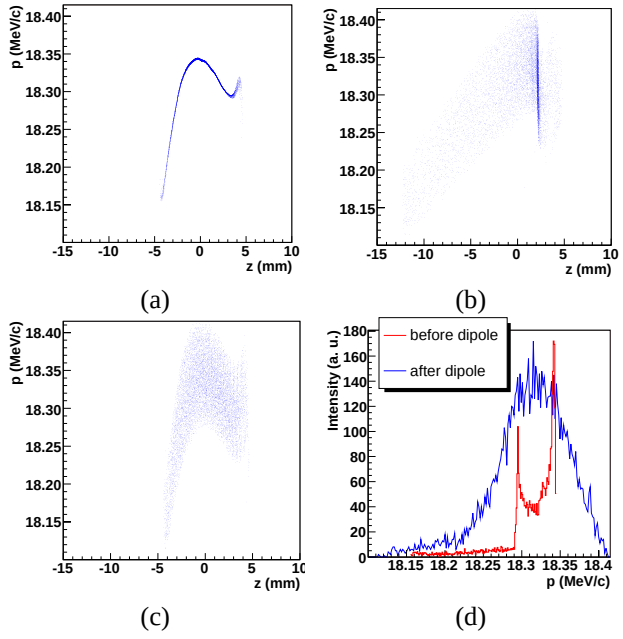

Figure 3: Longitudinal phase space obtained with the quadrupole magnet Q_2 being off: longitudinal phase space (a), reconstructed longitudinal phase space at S_1 (b), reconstructed longitudinal phase space at S_1 after correction of M_{56} (c), momentum distribution (d)

.

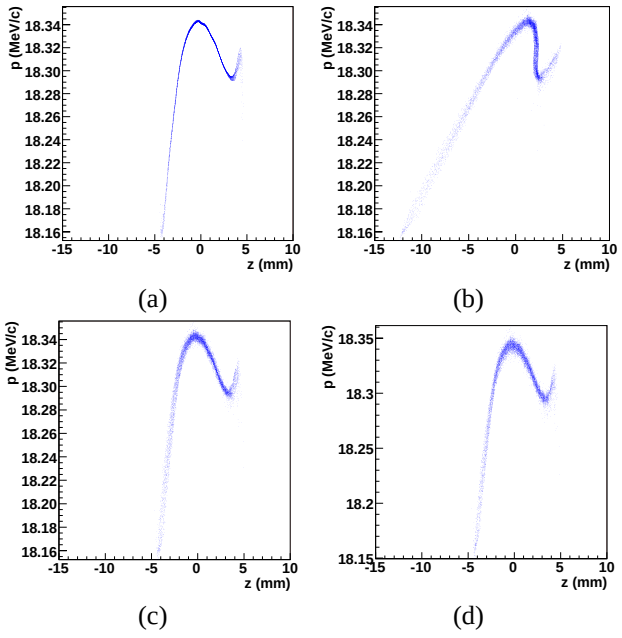

Figure 4: Longitudinal phase space obtained with the quadrupole triplet placed on the position of Q_2 being on: longitudinal phase space (a), reconstructed longitudinal phase space at S_1 (b), reconstructed longitudinal phase space at S_1 after correction of M_{56} (c). For a comparison reconstructed longitudinal phase space at S_1 [as (c)] but with a single quadrupole instead of a triplet.

beam onto screen S_1 (at position 6.5 m). The results are shown in figure 4 and following table .

	p_{mean} (MeV)	p_{rms} (keV)	ϵ_l (π keV mm)
(a)	18.3105	36.54	75.72
(c)	18.3104	36.59	76.11
$(a-c)/a$	-0.0005%	0.16%	0.5%

The use of a quadrupole triplet brings a remarkable improvement to the measurements of the longitudinal phase space. Both, the longitudinal phase space and the momentum distribution are reproduced with very good agreement. The differences between the simulated and reconstructed values of the momentum spread and longitudinal emittance reduces by using of the triplet from about 35% down to less than one per cent.

In order to save some space in the main beamline, we studied the possibility to exchange the quadrupole triplet with a single quadrupole magnet. Indeed such replacement almost does not decrease the accuracy of the longitudinal phase-space reconstruction. Figure 5 shows a comparison of the momentum measurements. The differences between the simulated and reconstructed mean momentum, momentum spread and longitudinal phase space are still within 1 %.

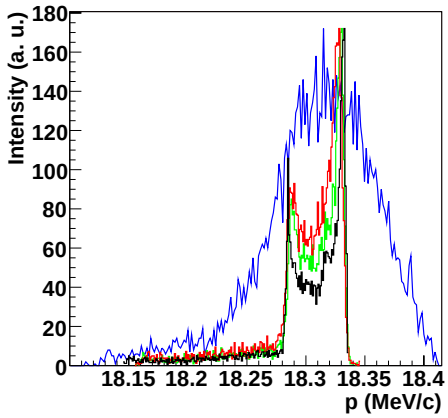

Figure 5: Simulated momentum distribution (black) compared to its reconstruction in the dispersive arm with the single quadrupole Q_2 (red), quadrupole triplet (green) and without quadrupole (blue).

TRANSVERSE SLICE EMITTANCE MEASUREMENTS

The functionality of the HEDA can be enhanced with a setup that allows us to measure the transverse emittance of the electron beam at different longitudinal positions along the bunch. The so called slice emittance is providing better understanding of the physics of a photoinjector, particulary the emittance compensation and conservation principles. It is also an important parameter for the SASE FELs since the slice emittance and slice peak current define the gain of the SASE FEL process. Using proper phasing of the booster cavity we can obtain linear correlation between the momentum and longitudinal distribution of the electrons in

the bunch. Afterwards one applies the standard quadrupole scan technique and measures the emittance for different momentum/time slices of the bunch.

A setup similar to that in [8] will be implemented. A slit at the dipole exit selects the necessary slice from the energy chirped beam. This slice is scanned with the quadrupole Q_1 focusing in a plane orthogonal to the dispersion plane of the dipole, the beam distribution will be observed on screen S_1. Due to the short distance between the quadrupole and the screen the beam size tends to become very small during the scan. For the correction of this the quadrupole magnet Q_2 with fixed strength placed before the dipole will be used (see Fig.1). The experimental setup was simulated with

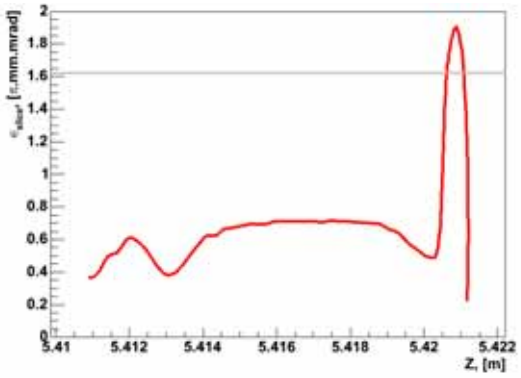

Figure 6: Slice emittance distribution at the dipole entrance. The solid line gives the value for the projected emittance.

ASTRA [7] in attempt to verify the technique and to optimize the setup. For the simulations presented here, a gun gradient of 60 MV/m and a phase of maximum acceleration in the gun, the current in the main solenoid was 385 A, and a booster phase of +70 degrees were chosen. This corresponds to a projected emittance of $1.6\ mm \cdot mrad$ (see Fig. 6), a mean momentum of 17 MeV/c and an RMS momentum spread of 1.4 MeV/c.

The electron bunch was separated in ten longitudinal slices which were scanned with ten different quadrupole strengths. The distribution is fited to a quadratic equation (2) where the corresponding beam parameters are obtained.

$$\langle x_s^2 \rangle = M_{11}^2 \cdot \langle x_0^2 \rangle + 2 \cdot M_{11} M_{12} \langle x_0 \cdot x_0' \rangle + M_{22}^2 \cdot \langle x_0'^2 \rangle \quad (2)$$

Here $\langle x_s^2 \rangle$ is the beam size coresponding to the particular strength of the quadrupole magnet, M_{11}, M_{12} and M_{22} are the elements of the transport matrix, functions of the quadrupole strength, $\langle x_0^2 \rangle$, $\langle x_0 \cdot x_0^{'} \rangle$ and $\langle x_0^{'2} \rangle$ are the initial beam parameters that need to be found. The corresponding value for the emittance then is calculated using Eq. 3.

$$\varepsilon_n = \beta\gamma \cdot \sqrt{\langle x_0^2 \rangle \cdot \langle x_0'^2 \rangle - \langle x_0 \cdot x_0' \rangle^2}. \quad (3)$$

Here $\langle x_0^2 \rangle$ and $\langle x_0'^2 \rangle$ are the rms dimensions of the beam in the so-called trace phase space and $\langle x_0 \cdot x_0' \rangle$ is the correlation between both.

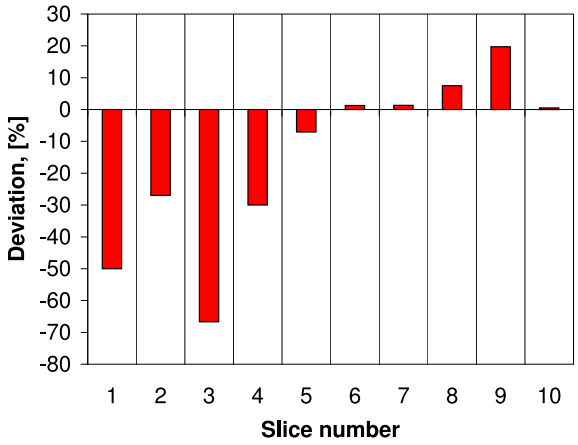

Figure 7: Deviation between the result from the simulated measurement and the slice emittance distribution obtained with ASTRA.

Figure 7 shows the deviation between the result from the simulated measurement and the slice emittance distribution obtained with ASTRA. The average deviation is 21 % but for some slices it can reach up to 66 %. Further improvement of the measuring accuracy can be reached by taking into account the space charge during the reconstruction.

ACKNOWLEDGEMENTS

Besides the funding agencies mentioned on the first page of the present paper the authors would like to thank S. Riemann, H.-J. Grabosch (both DESY) for valuable discussions. Without brilliant ideas of our engineers the realization of this work would not be thinkable.

REFERENCES

[1] F. Stephan, Status and perspectives of photo injector developments for high brightness beams, proceedings of teh workshop on the Physics and Applications of High Brightness Electron Beams. Erice, Italy, 2005.

[2] S. Korepanov et al., Design Consideration of the RF Deflector to Optimize the Photo Injector for PITZ, Proceedings of the FEL2006, Contribution THPPH021.

[3] D.J. Holder et al., A phase space tomography diagnostic for PITZ, Proceedings of EPAC 2006.

[4] D. Lipka, Spectrometer design for the SRF Gun, BESSY Note SRFgun-BESSY-003-12-2004, 2005.

[5] D. Lipka et al, Silica aerogel radiators for bunch length measurements, Nucl. Instr. Meth. A 538 (2005) 597.

[6] J. Rönsch et al., Measurement of the longitudinal phase space at the photo injector test facility at DESY in Zeuthen (PITZ), Proceedings of DIPAC 2005, Lyon.

[7] K.Floetmann, ASTRA, http://www.desy.de/ mpyflo.

[8] X. Qiu et al., Demonstration of emittance compensation through the measurement of the slice emittance of a 10 picosecond electron bunch, Phys. Rev. Let. 76 No. 20 (1996) 3723.